

Spectral Magnetization Ratchets with Discrete Time Quantum Walks

A. Mallick,¹ M. V. Fistul,^{1,2} P. Kaczynska,^{1,3} and S. Flach¹

¹*Center for Theoretical Physics of Complex Systems,
Institute for Basic Science (IBS), Daejeon 34126, Republic of Korea*

²*National University of Science and Technology "MISIS",
Russian Quantum Center, Moscow 119049, Russia*

³*Faculty of Physics, University of Warsaw, Warsaw 02-093, Poland*

(Dated: January 14, 2020)

We predict and theoretically study in detail the ratchet effect for the spectral magnetization of *periodic* discrete time quantum walks (DTQWs) — a repetition of a sequence of m different DTQWs. These generalized DTQWs are achieved by varying the corresponding coin operator parameters periodically with discrete time. We consider periods $m = 1, 2, 3$. The dynamics of m -periodic DTQWs is characterized by a two-band dispersion relation $\omega_{\pm}^{(m)}(k)$, where k is the wave vector. We identify a generalized parity symmetry of m -periodic DTQWs. The symmetry can be broken for $m = 2, 3$ by proper choices of the coin operator parameters. The obtained symmetry breaking results in a ratchet effect, i.e. the appearance of a nonzero spectral magnetization $M_s(\omega)$. This ratchet effect can be observed in the framework of continuous quantum measurements of the time-dependent correlation function of periodic DTQWs.

I. INTRODUCTION

Transport properties of particles and waves in spatially periodic structures that are driven by external time-dependent forces manifestly depend on the spacetime symmetries of the underlying equations of motion. A systematic analysis of these symmetries uncovers the conditions necessary for their violation and the appearance of the ratchet phenomenon to e.g. explain rectification of currents¹⁻⁴. Such phenomena have been predicted and studied in detail in various Hamiltonian and dissipative systems, for single particle⁵ and for many-body interacting systems⁶. Ratchets have been observed in various solid-state⁷, optical⁸, chemical and biological² systems.

Classical ratchet experimental platforms are modeled with a set of coupled nonlinear differential equations whose parameters vary in space and time. The ratchet effect results from broken spatio-temporal symmetries of the differential equations. Spatio-temporal symmetries typically involve discrete shift and parity operations⁴.

The quantum ratchet concept was predicted theoretically⁹⁻¹¹ and successfully implemented for a variety of different quantum systems platforms¹²⁻¹⁴. Quantum ratchets are typically described by quantum Hamiltonian systems which are periodically driven in time. The main body of studies was devoted to rectifying charge currents. An incoherent ratchet effect for driven and damped spins was reported in Refs.^{15,16}. To the best of our knowledge, spectral magnetization ratchets, i.e. frequency-selective magnetization ratchets for coherent non-dissipative quantum spin systems, were not considered so far.

To address the coherent quantum spin ratchet dynamics, we use the platform of discrete time quantum walks (DTQW)¹⁷. The DTQW is a spatio-temporal unitary map developed for quantum computing^{18,19}, which is obtained from a repeating sequence of coin and shift operators acting on a two-level (spin 1/2) system network. Re-

cently such platforms turned into a playground to study various interesting physical phenomena, e.g. single particle and many body Anderson localization²⁰⁻²², topological phenomena²³⁻²⁵, propagating solitons²⁶, relativistic Dirac particle systems²⁷⁻²⁹ etc. DTQWs have been experimentally implemented using ion-traps, photonic crystals, NMR³⁰, cavity-QED³¹ etc. DTQW ratchets³²⁻³⁴ were introduced for directed currents.

In order to obtain the spectral magnetization effect with DTQWs we introduce their generalization— m -periodic DTQWs — a repetition of a sequence of m different DTQWs. These generalized DTQWs are achieved by varying the corresponding coin operator parameters periodically as functions of the discrete time. We identify various symmetries of m -periodic DTQWs, and outline ways to break them for $m = 2, 3$. This ratchet effect can be observed in the framework of continuous quantum measurements of the time-dependent correlation function of periodic DTQWs.

The paper is organized as follows. We first introduce the model and dynamic equations for m -periodic DTQWs. We proceed with defining dispersion relations, eigenvectors, and magnetization properties. We continue to define the generalized parity symmetry. For $m = 1, 2, 3$ we analyze the conditions under which the generalized parity is broken, derive the symmetry breaking conditions, and obtain a spectral magnetization ratchet for $m = 2, 3$. Finally we discuss observation methods and conclude.

II. m -PERIODIC DISCRETE TIME QUANTUM WALKS

We consider a single particle m -periodic DTQW which is defined on a lattice of N sites. The quantum-mechanical dynamics of arbitrary DTQW is characterized by two-component wave functions $|\psi(n, t)\rangle =$

$(\psi_+(n, t), \psi_-(n, t))^T$ which depend on both site n and discrete time t . The discrete time-dependent probability amplitude for the whole system is characterized by the state $|\psi(t)\rangle = \sum_{n=1}^N |n\rangle \otimes |\psi(n, t)\rangle$. The m -periodic dynamics of such wave functions is determined by coin operators \hat{C}_ℓ , with the temporal index ℓ varying from 1 to m , and a shift operator, \hat{S} acting on the state as follows:

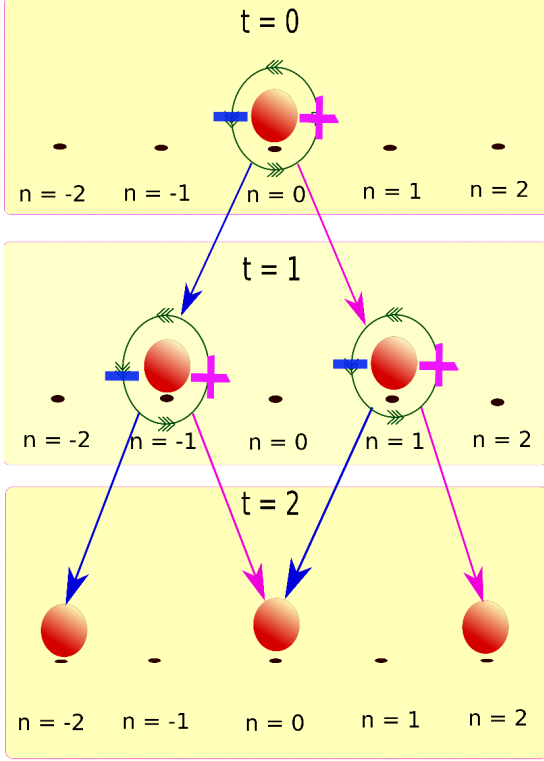


FIG. 1. Schematic representation of the 1-periodic DTQW. The lattice sites n are denoted by black dots, time flows from top to bottom following the arrows. The DTQW wavefunction $|\psi(n, t)\rangle$ is initialized at $t = 0$ and site $n = 0$ and evolves as denoted by straight arrows. The “ \pm ” signs indicate two spin-components (magenta (gray) and blue (light gray)). The double-arrow-decorated circles indicate coin operations which rotate the spin-components at each site. The straight arrows indicate the shift operations with the “ $+$ ” component shifted along the magenta (gray) arrow and the “ $-$ ” component along the blue (light gray) arrow.

$$|\psi(t + \ell)\rangle = \hat{S} \cdot \hat{C}_\ell |\psi(t + \ell - 1)\rangle, \quad \ell = 1, \dots, m. \quad (1)$$

We consider site-independent coin operators \hat{C}_ℓ :

$$\hat{C}_\ell = \mathbb{1} \otimes e^{i\varphi_\ell} \begin{pmatrix} e^{i\varphi_{1,\ell}} \cos \theta_\ell & e^{i\varphi_{2,\ell}} \sin \theta_\ell \\ -e^{-i\varphi_{2,\ell}} \sin \theta_\ell & e^{-i\varphi_{1,\ell}} \cos \theta_\ell \end{pmatrix}, \quad (2)$$

where $\mathbb{1}$ is the identity operator on position space, i.e. with rank N for a total number of N sites. The DTQW dynamics at each time t is determined by four angles: $\varphi, \varphi_1, \varphi_2, \theta$. These angles can be related to the action of

a potential energy, external and internal synthetic magnetic flux, and a kinetic energy, respectively²⁰. As outlined below, the potential energy angle φ turns irrelevant, and we will always set it to zero: $\varphi \equiv 0$. The shift operator couples neighboring sites by transferring the $\psi_+(n, t)$ components one step to the right, and the $\psi_-(n, t)$ components to the left:

$$\hat{S} = \sum_n |n\rangle \langle n+1| \otimes |-\rangle \langle -| + |n\rangle \langle n-1| \otimes |+\rangle \langle +|. \quad (3)$$

We then arrive at the generalized evolution operator of m -periodic DTQWs:

$$\hat{U}^{(m)} = \prod_{\ell=1}^m \hat{U}_\ell = \prod_{\ell=1}^m \hat{S} \cdot \hat{C}_\ell. \quad (4)$$

The schematic of the DTQW evolution is presented in Fig. 1.

Translational invariance of the evolution operator $\hat{U}_\ell = \hat{S} \cdot \hat{C}_\ell$ allows to apply Bloch's theorem and to expand the wave function in the plane wave basis as $|\psi(n, t)\rangle = \frac{1}{\sqrt{N}} \sum_k e^{ikn} |\psi(k, t)\rangle$ where $|\psi(k, t)\rangle = (\psi_+(k, t), \psi_-(k, t))^T$ is the two-component wave function in momentum space. The dynamics of an m -periodic DTQW in k -space follows as

$$|\psi(k, t + m)\rangle = \prod_{\ell=1}^m \hat{U}_\ell(k) |\psi(k, t)\rangle. \quad (5)$$

The evolution operator for a single m -period can be written as $\hat{U}^{(m)} = \sum_k |k\rangle \langle k| \otimes \hat{U}^{(m)}(k) = \sum_k |k\rangle \langle k| \otimes \prod_{\ell=1}^m \hat{U}_\ell(k)$ where

$$\hat{U}_\ell(k) = e^{i\varphi_\ell} \begin{pmatrix} e^{i\varphi_{1,\ell} - ik} \cos \theta_\ell & e^{i\varphi_{2,\ell} - ik} \sin \theta_\ell \\ -e^{-i\varphi_{2,\ell} + ik} \sin \theta_\ell & e^{-i\varphi_{1,\ell} + ik} \cos \theta_\ell \end{pmatrix}. \quad (6)$$

III. DISPERSION RELATIONS AND EIGENVECTORS

The solution of Eq. (5) is written as $|\psi(k, t)\rangle = e^{-i\omega^{(m)}t} |\psi(k, \omega^{(m)})\rangle$, where $|\psi(k, \omega^{(m)})\rangle = (\psi_+(k, \omega^{(m)}), \psi_-(k, \omega^{(m)}))^T$ is the corresponding two component wave function in momentum and frequency space. The frequency $\omega^{(m)}$ is a function of the momentum k and can take two values for fixed value of k , i.e. $\omega_\pm^{(m)}(k)$. This follows directly from having two levels (degrees of freedom) per lattice site (unit cell) which dictates a band structure with two bands. From Eqs. (5) and (6) it follows that nonzero values of the angles φ_ℓ result in a shift of $\omega_\pm^{(m)}$ only. This is similar to a potential which is constant in space and only shifts the energy of a quantum system. Therefore we set $\varphi_\ell = 0$ for all l .

The evolution operator

$$\hat{U}^{(m)}(k) = \prod_{\ell=1}^m \hat{U}_\ell(k) = \begin{pmatrix} u_{11}^{(m)} & u_{12}^{(m)} \\ -[u_{12}^{(m)}]^* & [u_{11}^{(m)}]^* \end{pmatrix} \quad (7)$$

is a unitary matrix, whose eigenvalues yield the dispersion relation of m -periodic DTQWs:

$$\omega_{\pm}^{(m)}(k) = \pm \frac{1}{m} \arccos \left(\Re \left[u_{11}^{(m)}(k) \right] \right). \quad (8)$$

For each value of the wave number k we find two frequencies with opposite values. Thus the band structure of any m -periodic DTQW is given by two bands which are symmetry related by (8). Because of Bloch's theorem, the matrix elements $u_{\alpha\beta}^{(m)}$ for all α, β in Eq. (7) are periodic functions of k . Hence $\omega_{\pm}^{(m)}(k)$ is also a periodic function of k . The corresponding eigenvectors are given by $|k\rangle \otimes |\psi(k, \omega_{\pm}^{(m)})\rangle$ with the spinor part

$$|\psi(k, \omega_{\pm}^{(m)})\rangle = \frac{\left(iu_{12}^{(m)}, \Im m \left[u_{11}^{(m)} \right] + \sin \left[m\omega_{\pm}^{(m)} \right] \right)^T}{\sqrt{\left| u_{12}^{(m)} \right|^2 + \left| \Im m \left[u_{11}^{(m)} \right] + \sin \left[m\omega_{\pm}^{(m)} \right] \right|^2}}. \quad (9)$$

IV. MAGNETIZATION

The magnetization of an eigenstate measures the population imbalance between the upper and lower levels. It is obtained from the expectation value of the magnetization operator $\hat{M} = \mathbf{1} \otimes \hat{\sigma}_3$ as

$$\begin{aligned} M_{\pm}(k) &= \langle \langle k | \mathbf{1} | k \rangle \langle \psi(k, \omega_{\pm}^{(m)}) | \hat{\sigma}_3 | \psi(k, \omega_{\pm}^{(m)}) \rangle \rangle \\ &\equiv |\psi_+(k, \omega_{\pm}^{(m)})|^2 - |\psi_-(k, \omega_{\pm}^{(m)})|^2. \end{aligned} \quad (10)$$

With Eqs. (9) and (10) it follows

$$M_{\pm}(k) = \frac{-\Im m[u_{11}^{(m)}(k)]}{\sin[m\omega_{\pm}^{(m)}(k)]} \equiv \mp \frac{\Im m[u_{11}^{(m)}(k)]}{\sqrt{1 - (\Re e[u_{11}^{(m)}(k)])^2}}. \quad (11)$$

Note that \pm refers to the upper respectively lower branch of the two band dispersion relation.

The above result (11) is quite remarkable and can be used for a number of conclusions. The magnetization of an eigenstate is entirely defined by the matrix element $u_{11}^{(m)}(k)$ of the evolution operator $\hat{U}^{(m)}(k)$, c.f. (7,8). It follows that the upper and lower branch magnetizations are opposite to each other: $M_+(k) = -M_-(k)$. Exciting a monochromatic (single wavelength) mix of states with one value of k and equal weights of eigenstates yields zero monochromatic magnetization

$$M_k = M_+(k) + M_-(k) = 0 \quad (12)$$

for any m -periodic DTQW. Thus also the total magnetization M_{tot} - the sum over the magnetization values for all eigenstates (with equal weight) vanishes pairwise for each k and is exactly zero for any m -periodic DTQW :

$$M_{tot} = \sum_k M_k = 0. \quad (13)$$

At variance to the above, the spectral magnetization $M_s(\omega)$ measures the average magnetization of all eigenstates with $\omega_{\pm}(k_l) = \omega$. Different eigenstates with identical frequency can be excited using spectroscopic methods, as we will show below. Due to the fact that $\Re e u_{11}(k)$ and consequently $\omega_{\pm}(k)$ are periodic functions of k , the spectral magnetization will average over a discrete set of eigenstates counted by the integer l :

$$M_s(\omega) = \sum_{k_l} M_{\pm}(k_l), \quad \omega = \omega_{\pm}(k_l). \quad (14)$$

For a fixed value of ω , the denominator in Eq.(11) is invariant for all allowed values of k_l . Further, since $\omega_{\pm}(k)$ is a periodic function in k , the set $\{k_l\}$ contains an even number of states. The rest of this work is devoted to answering the question, under which conditions a generalized parity symmetry will hold such that the set $\{k_l\}$ will have symmetry-related pairs of states for which the magnetization vanishes pairwise. The breaking of that generalized parity symmetry will then lead to a nonzero spectral magnetization. We coin this effect *spectral magnetization ratchet*.

V. GENERALIZED PARITY SYMMETRY

The spectral magnetization ratchet requires the breaking of the *generalized parity symmetry*. If the ratchet effect is absent, the m -periodic DTQW is invariant under the action of the generalized parity symmetry operation:

$$\hat{U}^{(m)} = (\mathcal{P} \otimes \mathcal{G}) \cdot \hat{U}^{(m)} \cdot (\mathcal{P} \otimes \mathcal{G})^\dagger, \quad (15)$$

where \mathcal{P} is an operator inducing reflection in momentum-space around some wave number K , and \mathcal{G} is an operator inducing spin flips with an additional phase shift G :

$$\begin{aligned} \mathcal{P} &= \sum_k |2K - k\rangle \langle k| = \sum_x e^{-2iKx} |-x\rangle \langle x|, \\ \mathcal{G} &= \begin{pmatrix} 0 & -e^{iG} \\ 1 & 0 \end{pmatrix}. \end{aligned} \quad (16)$$

If existing, the values of K and G will depend on the particular parameters of the m -periodic DTQW - hence the term *generalized parity*. In the presence of that symmetry, for each eigenstate $|k\rangle \otimes |\psi(k, \omega_{\pm}^{(m)})\rangle$ there exists another eigenstate $|2K - k\rangle \otimes |\psi(2K - k, \omega_{\pm}^{(m)})\rangle$, such that

$$\mathcal{G} |\psi(k, \omega_{\pm}^{(m)})\rangle = |\psi(k, \omega_{\mp}^{(m)})\rangle = |\psi(2K - k, \omega_{\pm}^{(m)})\rangle, \quad (17)$$

i.e. both states share the same eigenfrequency $\omega_{\pm}^{(m)}$. In terms of the matrix elements of the evolution operator $\hat{U}^{(m)}$ this symmetry implies

$$u_{11}^{(m)}(2K - k) = \left[u_{11}^{(m)}(k) \right]^*, \quad (18)$$

$$u_{12}^{(m)}(2K - k) = e^{iG} \left[u_{12}^{(m)}(k) \right]^*. \quad (19)$$

The consequence of (17) is $M_s(\omega) = 0$. Indeed, the parity operator \mathcal{G} swaps the spin components and therefore reverts the sign of the magnetization (12), which then leads to opposite magnetizations of $|\psi(k, \omega_{\pm}^{(m)})\rangle$ and $|\psi(2K - k, \omega_{\pm}^{(m)})\rangle$. In operator form the generalized parity symmetry (17),(18-19) can be expressed as

$$(\mathcal{P} \otimes \mathcal{G}) \cdot \hat{M} \cdot (\mathcal{P} \otimes \mathcal{G})^\dagger = -\hat{M}. \quad (20)$$

In order to realize the spectral magnetization ratchet effect, i.e. $M_s(\omega) \neq 0$, one needs to *break* the generalized parity symmetry Eq. (17-20). In the next section we explicitly show how to break the generalized parity symmetry and realize the ratchet effect for $m = 2, 3$ -periodic DTQWs.

VI. THE SPECTRAL MAGNETIZATION RATCHET

A. $m = 1$

For $m = 1$, the dispersion relation is written explicitly as²⁰

$$\omega_{\pm}^{(1)}(k) = \pm \arccos[\cos(\theta_1) \cos(k - \varphi_{1,1})]. \quad (21)$$

Typical two-band dispersion relations $\omega_{\pm}^{(1)}(k)$ for various values of θ_1 are shown in Fig. 2.

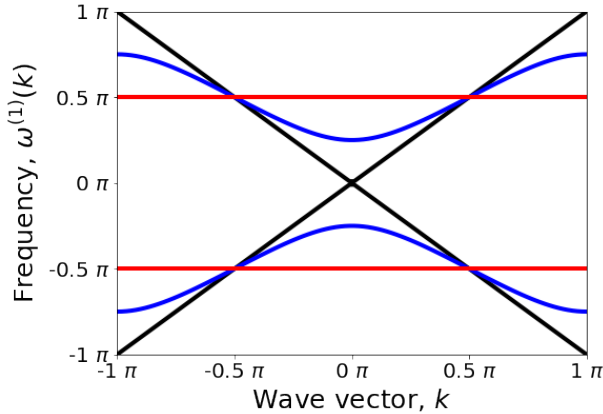


FIG. 2. Dispersion relation $\omega_{\pm}(k)$ for $m = 1$. $\theta_1 = 0$ (black solid lines), $\theta_1 = \pi/4$ (blue (light gray) solid lines) and $\theta_1 = \pi/2$ (red (gray) solid lines). Other parameters: $\varphi_{1,1} = \varphi_{2,1} = 0$.

With (6) we find

$$u_{11}^{(1)} = e^{i(\varphi_{1,1}-k)} \cos \theta_1, \quad (22)$$

$$u_{12}^{(1)} = e^{i(\varphi_{2,1}-k)} \sin \theta_1. \quad (23)$$

It follows that the generalized parity symmetry relations (18,19) are satisfied for all coin parameters of the DTQW with the notations $K = \varphi_{1,1}$ and $G = 2(\varphi_{2,1} - \varphi_{1,1})$.

Therefore the spectral magnetization $M_s(\omega) = 0$, and a single period DTQW always possesses generalized parity symmetry. This happens remarkably despite the action of both nonzero external and internal magnetic flux $\varphi_{1,1}$ and $\varphi_{2,1}$.

For the one-periodic DTQW all eigenstates are doubly degenerated, and using Eqs. (21) and (11) we obtain

$$M_+(k) = \frac{\cos(\theta_1) \sin(k - \varphi_{1,1})}{\sqrt{1 - \cos^2(\theta_1) \cos^2(k - \varphi_{1,1})}}. \quad (24)$$

In line with the above symmetry analysis the spectral magnetization vanishes, as also observed from the loop symmetry in Fig.3.

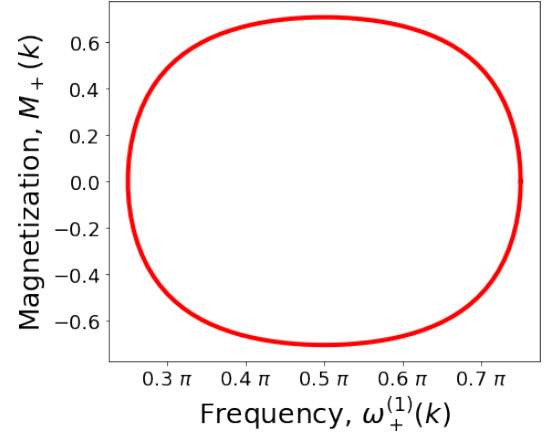


FIG. 3. Typical dependence of $M_+(k)$ from Eq.(24) which forms a symmetric loop around $M = 0$. The x -axis values of the frequency are obtained from Eq.(21). The spectral magnetization $M_s(\omega) = 0$. Here $\theta_1 = \pi/4$ and $\varphi_{1,1} = \varphi_{2,1} = 0$.

B. $m = 2$

For $m = 2$ we calculate the product of two operators $\hat{U}_1(k)$ and $\hat{U}_2(k)$ and find

$$\begin{aligned} u_{11}^{(2)} &= \cos(\theta_1) \cos(\theta_2) e^{-i(2k - \varphi_{1,1} - \varphi_{1,2})} \\ &\quad - \sin(\theta_1) \sin(\theta_2) e^{i(\varphi_{2,2} - \varphi_{2,1})}, \\ u_{12}^{(2)} &= \sin(\theta_1) \cos(\theta_2) e^{-i(2k - \varphi_{1,2} - \varphi_{2,1})} \\ &\quad + \cos(\theta_1) \sin(\theta_2) e^{-i(\varphi_{1,1} - \varphi_{2,2})}. \end{aligned} \quad (25)$$

With the help of Eqs. (7)-(8) we obtain the explicit expression for the dispersion relation $\omega_{\pm}^{(2)}(k)$ as

$$\begin{aligned} \omega_{\pm}^{(2)}(k) &= \pm \frac{1}{2} \arccos[\cos(\theta_1) \cos(\theta_2) \cos(2k - \varphi_{1,1} - \varphi_{1,2}) \\ &\quad - \sin(\theta_1) \sin(\theta_2) \cos(\varphi_{2,1} - \varphi_{2,2})]. \end{aligned} \quad (26)$$

Typical band structures are shown in Fig.4.

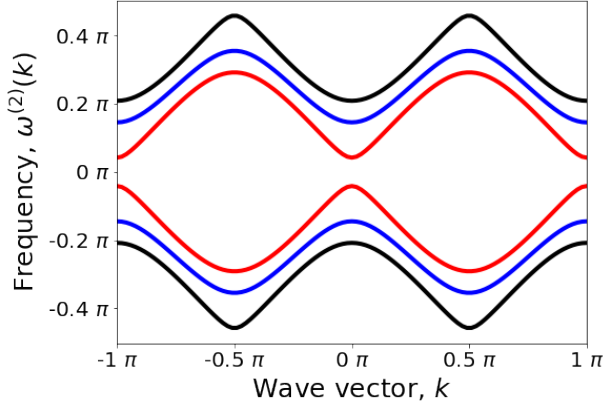


FIG. 4. Dispersion relation $\omega_{\pm}(k)$ for $m = 2$. $\varphi_{2,1} = 0$ (black solid lines); $\varphi_{2,1} = \pi/2$ (blue (light gray) line); $\varphi_{2,1} = \pi$ (red (gray) line). The other parameters are fixed to $\theta_1 = \pi/4$, $\theta_2 = \pi/6$, $\varphi_{1,1} = \varphi_{1,2} = \varphi_{2,2} = 0$.

In order to possess generalized parity symmetry (18,19), it follows from Eq.(25) that $\sin(\theta_1) \sin(\theta_2) e^{i(\varphi_{2,2} - \varphi_{2,1})} = 0$. Then it follows that

$$K = \frac{\varphi_{1,1} + \varphi_{1,2}}{2}. \quad (27)$$

Three symmetry cases can be distinguished.

$$S_{2,1} : \theta_1 = n\pi \rightarrow G = 2(\varphi_{2,2} - \varphi_{1,1}), \quad (28)$$

$$S_{2,2} : \theta_2 = n\pi \rightarrow G = -2(\varphi_{2,1} + \varphi_{1,1}), \quad (29)$$

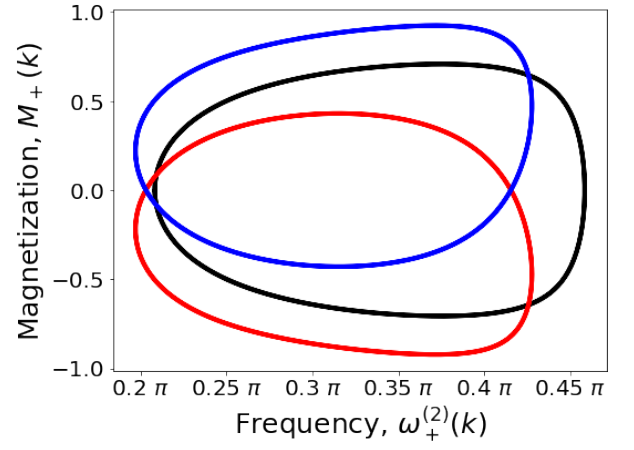
$$S_{2,3} : \varphi_{2,2} - \varphi_{2,1} = n\pi \rightarrow G = -2(\varphi_{2,1} + \varphi_{1,1}). \quad (30)$$

Here $n = 0, \pm 1, \pm 2, \dots$ is an arbitrary integer. If all of the above conditions are broken, then we can expect a nonzero spectral magnetization ratchet to appear. If on the contrary at least one of the above symmetry conditions $S_{2,1}, S_{2,2}, S_{2,3}$ is satisfied, the spectral magnetization vanishes for all frequencies.

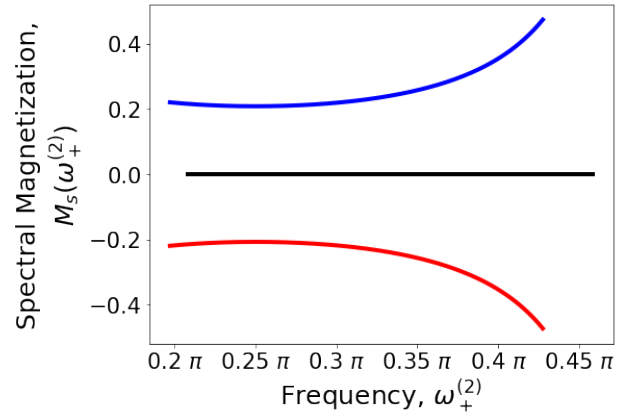
For the two-periodic DTQW the eigenstates are 4-fold degenerated, and using Eqs. (25) and (26) we obtain

$$M_+(k) = \frac{\cos(\theta_1) \cos(\theta_2) \sin(2k - 2k_0) - \sin(\theta_1) \sin(\theta_2) \sin(\delta\varphi_2)}{|\sin(2\omega_+^{(2)}(k))|}. \quad (31)$$

where $\delta\varphi_2 = \varphi_{2,1} - \varphi_{2,2}$, $k_0 = (\varphi_{1,1} + \varphi_{1,2})/2$. The typical dependencies of $M_+(k)$ for different values of phase shift $\delta\varphi_2$ are shown in Fig. 5. Nonzero spectral magnetization values appear once $\delta\varphi_2 \neq 0$, signaling the breaking of generalized parity symmetry (28-30) and the appearance of the spectral magnetization ratchet.



(a)



(b)

FIG. 5. (a) Typical dependencies of $M_+(k)$ versus $\omega_+^{(2)}(k)$. Black line (symmetric case) $\delta\varphi_2 = 0$; blue (light gray) line (non-symmetric case) $\delta\varphi_2 = \pi/5$; red (gray) line (non-symmetric case), $\delta\varphi_2 = -\pi/5$. Here $\theta_1 = \pi/4$, $\theta_2 = \pi/6$ and $\varphi_{1,1} = \varphi_{1,2} = 0$. (b) Spectral magnetization $M_s(\omega)$ for the corresponding plots of $M_+(k)$ from (a).

C. $m = 3$

For the 3-periodic DTQW we calculate the product of three operators $\hat{U}_1(k)$, $\hat{U}_2(k)$, $\hat{U}_3(k)$ and get

$$u_{11}^{(3)}(k) = \cos(\theta_1) \cos(\theta_2) \cos(\theta_3) e^{i(k_a - 3k)} - \sin(\theta_1) \sin(\theta_2) \cos(\theta_3) e^{i(k_b - k)} - \sin(\theta_1) \cos(\theta_2) \sin(\theta_3) e^{i(-k_c + k)} - \cos(\theta_1) \sin(\theta_2) \sin(\theta_3) e^{i(k_d - k)} \quad (32)$$

with the notations

$$k_a = \varphi_{1,1} + \varphi_{1,2} + \varphi_{1,3}, \quad (33)$$

$$k_b = \varphi_{1,3} - \varphi_{2,1} + \varphi_{2,2}, \quad (34)$$

$$k_c = \varphi_{1,2} + \varphi_{2,1} - \varphi_{2,3}, \quad (35)$$

$$k_d = \varphi_{1,1} - \varphi_{2,2} + \varphi_{2,3}. \quad (36)$$

Note that $k_a = k_b + k_c + k_d$. The off-diagonal element follows as

$$\begin{aligned} u_{12}^{(3)}(k) &= \sin(\theta_1) \cos(\theta_2) \cos(\theta_3) e^{i(k_e - 3k)} \\ &\quad + \cos(\theta_1) \sin(\theta_2) \cos(\theta_3) e^{i(k_f - k)} \\ &\quad + \cos(\theta_1) \cos(\theta_2) \sin(\theta_3) e^{i(-k_g + k)} \\ &\quad - \sin(\theta_1) \sin(\theta_2) \sin(\theta_3) e^{i(k_h - k)}. \end{aligned} \quad (37)$$

with the notations

$$k_e = \varphi_{1,2} + \varphi_{1,3} + \varphi_{2,1} = k_a + \varphi_{2,1} - \varphi_{1,1}, \quad (38)$$

$$k_f = -\varphi_{1,1} + \varphi_{1,3} + \varphi_{2,2} = k_b + \varphi_{2,1} - \varphi_{1,1}, \quad (39)$$

$$k_g = \varphi_{1,1} + \varphi_{1,2} - \varphi_{2,3} = k_c - \varphi_{2,1} + \varphi_{1,1}, \quad (40)$$

$$k_h = \varphi_{2,1} - \varphi_{2,2} + \varphi_{2,3} = k_d + \varphi_{2,1} - \varphi_{1,1}. \quad (41)$$

Using Eqs. (7)-(8) we obtain the explicit expression for the dispersion relation $\omega_{\pm}^{(3)}(k)$ as

$$\begin{aligned} \omega_{\pm}^{(3)}(k) &= \pm \frac{1}{3} \arccos[\cos(\theta_1) \cos(\theta_2) \cos(\theta_3) \cos(3k - k_a) \\ &\quad - \sin(\theta_1) \sin(\theta_2) \cos(\theta_3) \cos(k - k_b) \\ &\quad - \sin(\theta_1) \cos(\theta_2) \sin(\theta_3) \cos(k - k_c) \\ &\quad - \cos(\theta_1) \sin(\theta_2) \sin(\theta_3) \cos(k - k_d)]. \end{aligned} \quad (42)$$

Typical band structures are shown in Fig. 6.

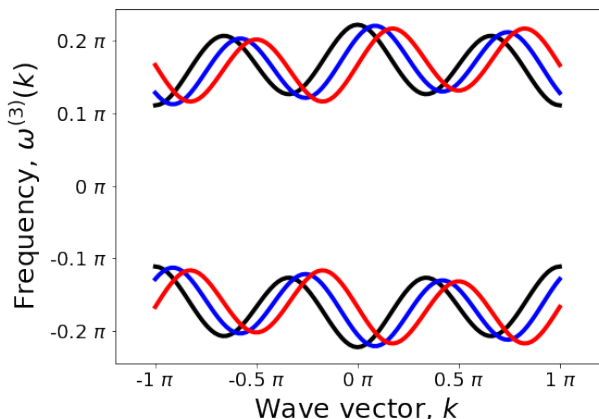


FIG. 6. Dispersion relation $\omega_{\pm}(k)$ for the three-periodic ($m = 3$) DTQW with different angles $\varphi_{1,1}$: symmetric case $\varphi_{1,1} = 0$ (black solid line); non-symmetric cases $\varphi_{1,1} = \pi/4$ (blue (light gray) line), $\varphi_{1,1} = \pi/2$ (red (gray) line). Here $\theta_1 = \pi/3$, $\theta_2 = \pi - 0.43$, $\theta_3 = 0.43$ are chosen. All other angles set to zero.

Let us identify parameters for which the generalized parity symmetry holds. We distinguish two symmetry conditions - $S_{3,1}$ and $S_{3,2}$. $S_{3,1}$ constrains the coin parameters θ_i , while leaving all other angles arbitrary:

$$S_{3,1} : \theta_i = n\pi/2, \theta_{j \neq i} = m\pi/2 \quad (43)$$

for arbitrary integers n, m . The details of the cumbersome analysis, including the values of K and G are outsourced to Appendix A.

The second generalized parity symmetry case $S_{3,2}$ constrains all but the coin parameters θ_i . It is realized when $k_a = 3k_b = 3k_c = 3k_d$ which implies $k_b = k_c = k_d$. These conditions reduce to

$$S_{3,2} : \begin{cases} \varphi_{2,2} = \frac{1}{3}(\varphi_{1,1} + \varphi_{1,2} - 2\varphi_{1,3}) + \varphi_{2,1} \\ \varphi_{2,3} = \frac{1}{3}(-\varphi_{1,1} + 2\varphi_{1,2} - \varphi_{1,3}) + \varphi_{2,1} \end{cases} \quad (44)$$

with the parameters of the generalized parity symmetry reading

$$K = k_b, G = 2(\varphi_{2,1} - \varphi_{1,1}). \quad (45)$$

If any of the two symmetries $S_{3,1}$ and $S_{3,2}$ holds, the spectral magnetization vanishes. If both are violated, a nonzero spectral magnetization ratchet is predicted.

Using Eqs. (32), (37), (42) and (11) we obtain the explicit expression for $M_+(k)$:

$$\begin{aligned} M_+(k) &= \left[\cos(\theta_1) \cos(\theta_2) \cos(\theta_3) \sin(3k - k_a) \right. \\ &\quad - \sin(\theta_1) \sin(\theta_2) \cos(\theta_3) \sin(k - k_b) \\ &\quad + \sin(\theta_1) \cos(\theta_2) \sin(\theta_3) \sin(k - k_c) \\ &\quad \left. - \cos(\theta_1) \sin(\theta_2) \sin(\theta_3) \sin(k - k_d) \right] \frac{1}{|\sin(3\omega_+^{(3)}(k))|}. \end{aligned} \quad (46)$$

We consider a case where all $\varphi_{i,j} = 0$ except $\varphi_{1,1}$, and $\theta_i \neq n\pi/2$ for any i and any integer n . The corresponding dispersion relation for such a case is shown in Fig. 6. From the previous analysis, it follows that the spectral magnetization must vanish if $\varphi_{1,1} = 0$ since then $S_{3,2}$ is restored. The dependence $M_+(k)$ for different values of the angle $\varphi_{1,1}$ is shown in Fig. 7a. Indeed the spectral magnetization $M_s(\omega) = 0$ is obtained if $\varphi_{1,1} = 0$ (see, black dotted line in Fig. 7b), as a direct consequence of the generalized parity symmetry with parameters $K = 0$, $G = 0$. For nonzero values of $\varphi_{1,1}$, the parity symmetry as described by Eq. (16) is broken, and non-zero values of spectral magnetization are obtained (see blue (light gray) and red (gray) line in Fig. 7).

VII. QUANTUM MEASUREMENTS OF THE SPECTRAL MAGNETIZATION RATCHET EFFECT

Let us discuss ways to observe the spectral magnetization $M_s(\omega)$ in the quantum evolution of m -periodic DTQWs. We introduce the time-dependent correlation function

$$C_M(t, \tau) = \sum_n \psi_+(n, t) \psi_+^*(n, t - \tau) - \psi_-(n, t) \psi_-^*(n, t - \tau), \quad (47)$$

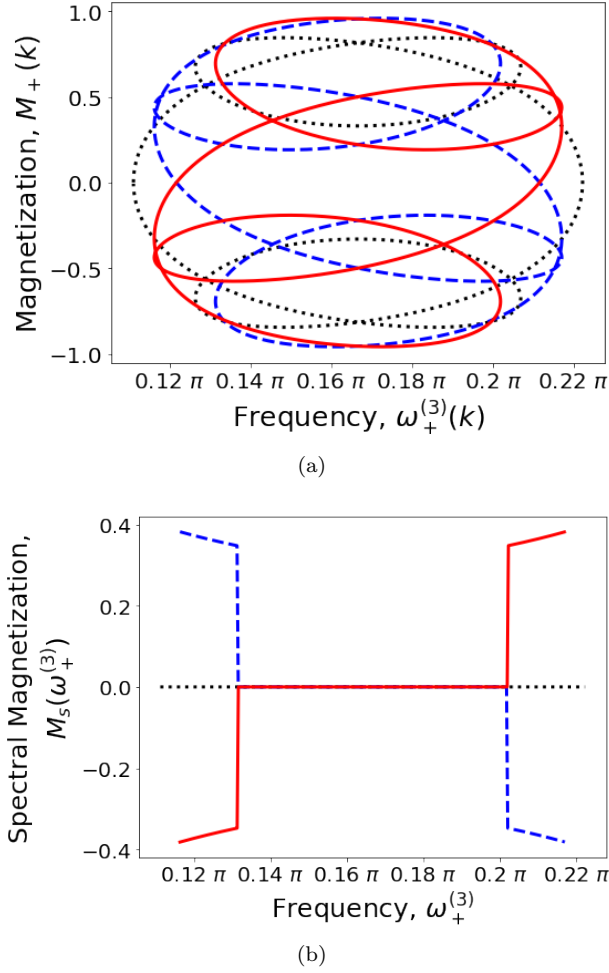


FIG. 7. (a) $M_+^{(3)}(k)$ as a function of frequency $\omega_+^{(3)}(k)$ for different values of $\delta\varphi_{1,1}$: black dotted line (symmetric case) $\varphi_{1,1} = 0$; blue (light gray) dashed line (non-symmetric case) $\varphi_{1,1} = \pi/2$; red (gray) solid line (non-symmetric case) $\varphi_{1,1} = -\pi/2$; Here $\theta_1 = \pi/3$, $\theta_2 = \pi - 0.43$, $\theta_3 = 0.43$, and $\varphi_{1,2} = \varphi_{1,3} = \varphi_{2,1} = \varphi_{2,2} = \varphi_{2,3} = 0$. (b) Spectral magnetization $M_s(\omega)$ for the corresponding plots of $M_+(k)$ in (a).

where we consider the time-steps t , τ as multiples of m . Its discrete Fourier-transformation w.r.t. τ with additional averaging over the discrete time t

$$C_M(\omega) = \sum_{\tau=0}^{\infty} e^{i\omega\tau} \left[\lim_{T \rightarrow \infty} \frac{1}{T} \sum_{t=0}^T C_M(t, \tau) \right] \quad (48)$$

can be expressed as

$$C_M(\omega) = \sum_l |\alpha(k_l, \omega)|^2 M(k_l), \quad (49)$$

where the index l in this sum runs over all degenerate points corresponding to the frequency ω . Note here that T is also a multiple of m . The coefficients $\alpha(k_l, \omega)$ are

determined by the initial conditions:

$$\psi_{\pm}(n, t=0) = \frac{1}{\sqrt{N}} \sum_k \sum_{p=\pm} e^{ikn} \alpha(k, \omega_p) \psi_{\pm}(k, \omega_p). \quad (50)$$

Assuming a homogeneous distribution of such coefficients $\alpha(k, \omega)$ such that $|\alpha(k, \omega)|^2 = \text{const}$, we obtain $C_M(\omega) \propto M_s(\omega)$ (see derivation details in Appendix B). Note that the assumption of all basis states having the same weight is similar to a generalized notion of infinite temperature. It follows that the infinite temperature states of quantum Floquet systems like in the case of m -periodic DTQWs may keep a nontrivial internal structure characterized by the presence or absence of certain symmetries.

The correlator $C_M(\omega)$ can be directly measured using a continuous quantum measurements setup proposed and regularly used for the study of quantum dynamics of superconducting qubit networks^{35–37}. These setups consist of a low-dissipative transmission line weakly coupled with the studied quantum system (here the DTQW). The transmission line is characterized by a discrete set of internal mode frequencies at which the transmission coefficient is suppressed. Let us consider one such mode with frequency ω_0 . Due to the additional coupling of the line with the DTQW the transmission coefficient $D(\omega)$ will display a resonant drop at the resonant frequency ω_{res} :

$$D(\omega) = 1 - \frac{\alpha}{(\omega - \omega_{res})^2 + \gamma^2}, \quad (51)$$

where α is the strength of the resonance and $\gamma \ll \omega$ is the dissipation parameter. The location of the resonance ω_{res} is renormalized due to the presence of the weakly coupled DTQW: $\omega_{res} = \omega_0 + \chi C_M(\omega_0)$, where χ is determined by the small coupling strength between the waveguide and the DTQW. Therefore, this method allows to measure the value of $C_M(\omega)$, and consequently allows to observe the predicted appearance of the spectral magnetization ratchet.

VIII. CONCLUSION

We have shown that a spectral magnetization ratchet can be observed in a spatially homogeneous DTQW system by breaking a generalized parity symmetry. To achieve that goal, we need to introduce a generalized discrete time quantum walk process with quantum coins varying periodically in time. As a result, we obtained conditions for the generalized parity symmetry to hold for $m = 2$ and $m = 3$, and identified systematic ways to break this symmetry by proper parameter choices. As a result, a non-vanishing spectral magnetization is obtained, which tells that a resonant excitation of all (degenerate) eigenstates at a given eigenfrequency ω will lead to a non-vanishing population imbalance, or simply magnetization. Our results add new possibilities to

the control of quantum networks in quantum simulation setups using methods developed in condensed matter physics.

ACKNOWLEDGMENT

This work was supported by the Institute for Basic Science, Project Code (IBS-R024-D1). P. K. thanks the hos-

pitality of the Center for Theoretical Physics of Complex Systems and the Korean Undergraduate Science Program KUSP2019 (kusp.ibs.re.kr) at the Institute for Basic Science for hospitality and financial support. M. V. F. thanks the partial financial support of Ministry of Science and Higher Education of the Russian Federation in the framework of Increase Competitiveness Program of NUST 'MISiS' K2-2017-081.

-
- ¹ P. Reimann, Brownian motors: noisy transport far from equilibrium, *Physics Reports* **361**, 57265 (2002).
 - ² F. Julicher, A. Ajdari, and J. Prost, Modeling molecular motors, *Reviews of Modern Physics* **69**, 1269 (1997).
 - ³ P. Hanggi, F. Marchesoni, and F. Nori, Brownian motors, *Annalen der Physik* **14**, 5170 (2005).
 - ⁴ S. Denisov, S. Flach, and P. Hanggi, Tunable transport with broken spacetime symmetries, *Physics Reports* **538**, 77120 (2014).
 - ⁵ S. Flach, O. Yevtushenko, and Y. Zolotaryuk, Directed current due to broken time-space symmetry, *Physical review letters* **84**, 2358 (2000).
 - ⁶ S. Flach, Y. Zolotaryuk, A. E. Mirosh-nichenko, and M. V. Fistul, Broken symmetries and directed collective energy transport in spatially extended systems, *Physical review letters* **88**, 184101 (2002).
 - ⁷ G. Carapella and G. Costabile, Ratchet effect: Demonstration of a relativistic fluxon diode, *Physical review letters* **87**, 077002 (2001).
 - ⁸ Chi Zhang, Chuan-Feng Li, and Guang-Can Guo, Experimental demonstration of photonic quantum ratchet, *Science Bulletin* **60**, 249255 (2015).
 - ⁹ P. Reimann, M. Grifoni, and P. Hanggi, Quantum ratchets, *Physical review letters* **79**, 10 (1997).
 - ¹⁰ S. Denisov, L. Morales-Molina, and S Flach, Quantum resonances and rectification in ac-driven ratchets, *EPL (Europhysics Letters)* **79**, 10007 (2007).
 - ¹¹ S. Denisov, L. Morales-Molina, S. Flach, and P. Hanggi, Periodically driven quantum ratchets: Symmetries and resonances, *Physical Review A* **75**, 063424 (2007).
 - ¹² J. B. Majer, J. Peguiron, M. Grifoni, M. Tusveld, and J. E. Mooij, Quantum ratchet effect for vortices, *Physical review letters* **90**, 056802 (2003).
 - ¹³ T. Salger, S. Kling, T. Hecking, C. Geckeler, L. M. Molina, and M. Weitz, Directed transport of atoms in a hamiltonian quantum ratchet, *Science* **326**, 12411243 (2009).
 - ¹⁴ C. Drexler, S. A. Tarasenko, P. Olbrich, J. Karch, M. Hirmer, F. Muller, M. Gmitra, J. Fabian, R. Yakimova, S. Lara-Avila, et al., Magnetic quantum ratchet effect in graphene, *Nature nanotechnology* **8**, 104 (2013).
 - ¹⁵ S. Flach and A. A. Ovchinnikov, Static magnetization induced by time-periodic fields with zero mean, *Physica A: Statistical Mechanics and its Applications* **292**, 268276 (2001).
 - ¹⁶ S. Flach, A. E. Miroshnichenko, and A. A. Ovchinnikov, ac-driven quantum spins: Resonant enhancement of transverse dc magnetization, *Phys. Rev. B* **65**, 104438 (2002).
 - ¹⁷ Y. Aharonov, L. Davidovich, and N. Zagury, Quantum random walks, *Phys. Rev. A* **48**, 1687 (1993).
 - ¹⁸ N. B. Lovett, S. Cooper, M. Everitt, M. Trevers, and V. Kendon, Universal quantum computation using the discrete-time quantum walk, *Phys. Rev. A* **81**, 042330 (2010).
 - ¹⁹ S. Singh, P. Chawla, A. Sarkar, C. M. Chandrashekar, Computational power of single qubit discrete-time quantum walk, [arXiv:1907.04084 \[quant-ph\]](https://arxiv.org/abs/1907.04084)(2019).
 - ²⁰ I. Vakulchyk, M. V. Fistul, P. Qin, and S. Flach, Anderson localization in generalized discrete-time quantum walks, *Phys. Rev. B* **96**, 144204 (2017).
 - ²¹ A. Crespi, R. Osellame, R. Ramponi, V. Giovannetti, R. Fazio, L. Sansoni, F. D. Nicola, F. Sciarrino and P. Matalon, Anderson localization of entangled photons in an integrated quantum walk, *Nature Photonics* **7**, 322 (2013)
 - ²² I. Vakulchyk, M. V. Fistul, and S. Flach, Wave packet spreading with disordered nonlinear discrete-time quantum walks, *Phys. Rev. Lett.* **122**, 040501 (2019).
 - ²³ T. Kitagawa, M. S. Rudner, E. Berg, and E. Demler, Exploring topological phases with quantum walks, *Phys. Rev. A* **82**, 033429 (2010).
 - ²⁴ J. K. Asboth, Symmetries, topological phases, and bound states in the one-dimensional quantum walk, *Phys. Rev. B* **86**, 195414 (2012).
 - ²⁵ T. Rakovszky and J. K. Asboth, Localization, delocalization, and topological phase transitions in the one-dimensional split-step quantum walk, *Phys. Rev. A* **92**, 052311 (2015).
 - ²⁶ M. Maeda, H. Sasaki, E. Segawa, A. Suzuki and K. Suzuki, Dynamics of solitons for nonlinear quantum walks, *J. Phys. Commun.* **3**, 075002 (2019).
 - ²⁷ A. Mallick and C. M. Chandrashekar, Dirac cellular automaton from split-step quantum walk, *Sci. Rep.* **6**, 25779 (2016).
 - ²⁸ A. Mallick, S. Mandal, A. Karan, and C. M. Chandrashekar, Simulating dirac hamiltonian in curved space-time by split-step quantum walk, *Journal of Physics Communications* **3**, 015012 (2019).
 - ²⁹ P. Arnault, A. Prez, P. Arrighi, and T. Farrelly, Discrete-time quantum walks as fermions of lattice gauge theory, *Phys. Rev. A* **99**, 032110 (2019).
 - ³⁰ J. Du, Hui Li, X. Xu, M. Shi, Jihui Wu, Xianyi Zhou, and R. Han, Experimental implementation of the quantum random-walk algorithm, *Phys. Rev. A* **67**, 042316 (2003).
 - ³¹ T. Di, M. Hillery, and M. S. Zubairy, Cavity QED-based quantum walk, *Phys. Rev. A* **70**, 032304 (2004).
 - ³² D. A. Meyer, Noisy quantum parrondo games, Fluctuations and Noise in Photonics and Quantum Optics, *Proc. SPIE* **5111** (2003).

- ³³ S. Chakraborty, A. Das, A. Mallick, and C. M. Chandrashekar, Quantum Ratchet in Disordered Quantum Walk, *Annalen der Physik* **529**, 1600346 (2017).
- ³⁴ J. Rajendran and C. Benjamin, Playing a true Parrondo's game with a three-state coin on a quantum walk, *EPL (Europhysics Letters)*, **122**, 4 (2018).
- ³⁵ A. Wallraff, D. I. Schuster, A. Blais, L. Frunzio, R. S. Huang, J. Majer, S. Kumar, S. M. Girvin, and R. J. Schoelkopf, Strong coupling of a single photon to a superconducting qubit using circuit quantum electrodynamics, *Nature* **431**, 162 (2004).
- ³⁶ P. A. Volkov and M. V. Fistul, Collective quantum coherent oscillations in a globally coupled array of superconducting qubits, *Physical Review B* **89**, 054507 (2014).
- ³⁷ P. Macha, G. Oelsner, J. M. Reiner, M. Marthaler, S. Andre, G. Schon, U. Hubner, H. G. Meyer, E. Il'ichev, and A. V. Ustinov, Implementation of a quantum metamaterial using superconducting qubits, *Nature communications* **5**, 5146 (2014).

Appendix A: Symmetry $S_{3,1}$ for $m = 3$

Here we analyse the generalized parity symmetry $S_{3,1}$ which holds when $\theta_i = n\pi/2$ and $\theta_j = m\pi/2$ is satisfied for any pair of $i \neq j$. In the following n, m are arbitrary integers.

1. $i = 1, j = 2$

- For $\theta_1 = (2n + 1)\frac{\pi}{2}$, $\theta_2 = m\pi$, we have

$$\begin{aligned} u_{11}^{(3)}(k) &= -(-1)^{m+n} \sin(\theta_3) e^{i(-k_c+k)}, \\ u_{12}^{(3)}(k) &= (-1)^{m+n} \cos(\theta_3) e^{i(k_e-3k)} \\ \Rightarrow u_{11}^{(3)}(2k_c - k) &= \left[u_{11}^{(3)}(k) \right]^*, \\ u_{12}^{(3)}(2k_c - k) &= e^{2i(k_e-3k_c)} \left[u_{12}^{(3)}(k) \right]^*. \end{aligned} \quad (\text{A1})$$

$$\Rightarrow K = k_c, G = 2(k_e - 3k_c). \quad (\text{A2})$$

- For $\theta_1 = n\pi$, $\theta_2 = m\pi$, we have

$$\begin{aligned} u_{11}^{(3)}(k) &= (-1)^{m+n} \cos(\theta_3) e^{i(k_a-3k)}, \\ u_{12}^{(3)}(k) &= (-1)^{m+n} \sin(\theta_3) e^{i(-k_g+k)} \\ \Rightarrow u_{11}^{(3)}(2k_a/3 - k) &= \left[u_{11}^{(3)}(k) \right]^*, \\ u_{12}^{(3)}(2k_a/3 - k) &= e^{2ik_a/3 - 2ik_g} \left[u_{12}^{(3)}(k) \right]^*, \end{aligned} \quad (\text{A3})$$

$$\Rightarrow K = k_a/3, G = 2k_a/3 - 2k_g. \quad (\text{A4})$$

- For $\theta_1 = n\pi$, $\theta_2 = (2m + 1)\frac{\pi}{2}$, we have

$$\begin{aligned} u_{11}^{(3)}(k) &= -(-1)^{m+n} \sin(\theta_3) e^{i(k_d-k)}, \\ u_{12}^{(3)}(k) &= (-1)^{m+n} \cos(\theta_3) e^{i(k_f-k)} \\ \Rightarrow u_{11}^{(3)}(2k_d - k) &= \left[u_{11}^{(3)}(k) \right]^*, \\ u_{12}^{(3)}(2k_d - k) &= e^{2i(k_f-k_d)} \left[u_{12}^{(3)}(k) \right]^*. \end{aligned} \quad (\text{A5})$$

$$\Rightarrow K = k_d, G = 2(k_f - k_d). \quad (\text{A6})$$

- For $\theta_1 = (2n + 1)\frac{\pi}{2}$, $\theta_2 = (2m + 1)\frac{\pi}{2}$, we have

$$\begin{aligned} u_{11}^{(3)}(k) &= -(-1)^{m+n} \cos(\theta_3) e^{i(k_b-k)}, \\ u_{12}^{(3)}(k) &= -(-1)^{m+n} \sin(\theta_3) e^{i(k_h-k)} \\ \Rightarrow u_{11}^{(3)}(2k_b - k) &= \left[u_{11}^{(3)}(k) \right]^*, \\ u_{12}^{(3)}(2k_b - k) &= e^{2i(k_h-k_b)} \left[u_{12}^{(3)}(k) \right]^*. \end{aligned} \quad (\text{A7})$$

$$\Rightarrow K = k_b, G = 2(k_h - k_b). \quad (\text{A8})$$

2. $i = 1, j = 3$

- For $\theta_1 = (2n + 1)\frac{\pi}{2}$, $\theta_3 = m\pi$, we have

$$\begin{aligned} u_{11}^{(3)}(k) &= -(-1)^{m+n} \sin(\theta_2) e^{i(k_b-k)}, \\ u_{12}^{(3)}(k) &= (-1)^{m+n} \cos(\theta_2) e^{i(k_e-3k)} \\ \Rightarrow u_{11}^{(3)}(2k_b - k) &= \left[u_{11}^{(3)}(k) \right]^*, \\ u_{12}^{(3)}(2k_b - k) &= e^{2i(k_e-3k_b)} \left[u_{12}^{(3)}(k) \right]^* \end{aligned} \quad (\text{A9})$$

$$\Rightarrow K = k_b, G = 2(k_e - 3k_b). \quad (\text{A10})$$

- For $\theta_1 = n\pi$, $\theta_3 = m\pi$, we have

$$\begin{aligned} u_{11}^{(3)}(k) &= (-1)^{m+n} \cos(\theta_2) e^{i(k_a-3k)}, \\ u_{12}^{(3)}(k) &= (-1)^{m+n} \sin(\theta_2) e^{i(k_f-k)} \\ \Rightarrow u_{11}^{(3)}(2k_a/3 - k) &= \left[u_{11}^{(3)}(k) \right]^*, \\ u_{12}^{(3)}(2k_a/3 - k) &= e^{2ik_f - 2ik_a/3} \left[u_{12}^{(3)}(k) \right]^*. \end{aligned} \quad (\text{A11})$$

$$K = k_a/3, G = 2k_f - 2k_a/3. \quad (\text{A12})$$

- For $\theta_1 = n\pi$, $\theta_3 = (2m + 1)\frac{\pi}{2}$, we have

$$\begin{aligned} u_{11}^{(3)}(k) &= -(-1)^{m+n} \sin(\theta_2) e^{i(k_d-k)}, \\ u_{12}^{(3)}(k) &= (-1)^{m+n} \cos(\theta_2) e^{i(-k_g+k)} \\ \Rightarrow u_{11}^{(3)}(2k_d - k) &= \left[u_{11}^{(3)}(k) \right]^*, \\ u_{12}^{(3)}(2k_d - k) &= e^{-2i(k_g-k_d)} \left[u_{12}^{(3)}(k) \right]^*. \end{aligned} \quad (\text{A13})$$

$$K = k_d, G = -2(k_g - k_d). \quad (\text{A14})$$

- For $\theta_1 = (2n+1)\frac{\pi}{2}$, $\theta_3 = (2m+1)\frac{\pi}{2}$, we have

$$\begin{aligned} u_{11}^{(3)}(k) &= -(-1)^{m+n} \cos(\theta_2) e^{i(-k_c+k)}, \\ u_{12}^{(3)}(k) &= -(-1)^{m+n} \sin(\theta_2) e^{i(k_h-k)} \\ &\Rightarrow u_{11}^{(3)}(2k_c - k) = \left[u_{11}^{(3)}(k) \right]^*, \\ u_{12}^{(3)}(2k_c - k) &= e^{2i(k_h-k_c)} \left[u_{12}^{(3)}(k) \right]^* \end{aligned} \quad (\text{A15})$$

$$K = k_c, G = 2(k_h - k_c). \quad (\text{A16})$$

3. $i = 2, j = 3$

- For $\theta_2 = (2n+1)\frac{\pi}{2}$, $\theta_3 = m\pi$, we have

$$\begin{aligned} u_{11}^{(3)}(k) &= -(-1)^{m+n} \sin(\theta_1) e^{i(k_b-k)}, \\ u_{12}^{(3)}(k) &= (-1)^{m+n} \cos(\theta_1) e^{i(k_f-k)}, \\ &\Rightarrow u_{11}^{(3)}(2k_b - k) = \left[u_{11}^{(3)}(k) \right]^*, \\ u_{12}^{(3)}(2k_b - k) &= e^{2i(k_f-k_b)} \left[u_{12}^{(3)}(k) \right]^*. \end{aligned} \quad (\text{A17})$$

$$K = k_b, G = 2(k_f - k_b). \quad (\text{A18})$$

- For $\theta_2 = n\pi$, $\theta_3 = m\pi$, we have

$$\begin{aligned} u_{11}^{(3)}(k) &= (-1)^{m+n} \cos(\theta_1) e^{i(k_a-3k)}, \\ u_{12}^{(3)}(k) &= (-1)^{m+n} \sin(\theta_1) e^{i(k_e-3k)}, \\ &\Rightarrow u_{11}^{(3)}(2k_a/3 - k) = \left[u_{11}^{(3)}(k) \right]^*, \\ u_{12}^{(3)}(2k_a/3 - k) &= e^{2i(k_e-k_a)} \left[u_{12}^{(3)}(k) \right]^*. \end{aligned} \quad (\text{A19})$$

$$K = k_a/3, G = 2(k_e - k_a). \quad (\text{A20})$$

- For $\theta_2 = n\pi$, $\theta_3 = (2m+1)\frac{\pi}{2}$, we have

$$\begin{aligned} u_{11}^{(3)}(k) &= -(-1)^{m+n} \sin(\theta_1) e^{i(-k_c+k)}, \\ u_{12}^{(3)}(k) &= (-1)^{m+n} \cos(\theta_1) e^{i(-k_g+k)}, \\ &\Rightarrow u_{11}^{(3)}(2k_c - k) = \left[u_{11}^{(3)}(k) \right]^*, \\ u_{12}^{(3)}(2k_c - k) &= e^{2i(k_c-k_g)} \left[u_{12}^{(3)}(k) \right]^*. \end{aligned} \quad (\text{A21})$$

$$K = k_c, G = 2(k_c - k_g). \quad (\text{A22})$$

- For $\theta_2 = (2n+1)\frac{\pi}{2}$, $\theta_3 = (2m+1)\frac{\pi}{2}$, we have

$$\begin{aligned} u_{11}^{(3)}(k) &= -(-1)^{m+n} \cos(\theta_1) e^{i(k_d-k)}, \\ u_{12}^{(3)}(k) &= -(-1)^{m+n} \sin(\theta_1) e^{i(k_h-k)}, \\ &\Rightarrow u_{11}^{(3)}(2k_d - k) = \left[u_{11}^{(3)}(k) \right]^*, \\ u_{12}^{(3)}(2k_d - k) &= e^{2i(k_h-k_d)} \left[u_{12}^{(3)}(k) \right]^*. \end{aligned} \quad (\text{A23})$$

$$K = k_d, G = 2(k_h - k_d). \quad (\text{A24})$$

Appendix B: Derivation of the relation between the discrete time-dependent correlation function and the spectral magnetization

We consider all time intervals as multiples of m , so that $t, \tau \in m\mathbb{Z}$.

The expectation value of the operator: $(U^{(m)})^{\tau/m} \cdot \hat{M}$ w.r.t. a general state $|\psi(t)\rangle$ at time-step t can be written as

$$\begin{aligned} &\text{Tr} \left[|\psi(t)\rangle \langle \psi(t)| \cdot \left(U^{(m)} \right)^{\tau/m} \cdot \hat{M} \right] \\ &= \text{Tr} \left[|\psi(t)\rangle \langle \psi(t-\tau)| \cdot \hat{M} \right] \\ &= \sum_n \left\{ \langle n| \otimes \langle +| \right. |\psi(t)\rangle \langle \psi(t-\tau)| \cdot \hat{M} |n\rangle \otimes |+\rangle \left. \right\} \\ &\quad + \left\{ \langle n| \otimes \langle -| \right. |\psi(t)\rangle \langle \psi(t-\tau)| \cdot \hat{M} |n\rangle \otimes |-\rangle \left. \right\} \\ &= \sum_n \psi_+(n, t) \psi_+^*(n, t-\tau) - \psi_-(n, t) \psi_-^*(n, t-\tau). \end{aligned} \quad (\text{B1})$$

The last expression in the Eq. (B1) is denoted by $C_M(t, \tau)$ in the main text.

We write a general initial state as a superposition of orthogonal basis states (composite states of momentum basis and coin basis):

$$|\psi(t=0)\rangle = \sum_k \sum_{p=\pm} \alpha(k, \omega_p(k)) |k\rangle \otimes |\psi(k, \omega_p(k))\rangle \quad (\text{B2})$$

$$\begin{aligned} &\Rightarrow \psi_{\pm}(n, t=0) = \langle n, \pm | \psi(t=0) \rangle \\ &= \sum_k \sum_{p=\pm} \langle n|k\rangle \alpha(k, \omega_p(k)) \psi_{\pm}(k, \omega_p(k)) \\ &= \frac{1}{\sqrt{N}} \sum_k \sum_{p=\pm} e^{ikn} \left[\alpha(k, \omega_p(k)) \psi_{\pm}(k, \omega_p(k)) \right] \end{aligned} \quad (\text{B3})$$

with N being the number of lattice sites, so that

$$|k\rangle = \frac{1}{\sqrt{N}} \sum_n e^{ikn} |n\rangle \Rightarrow \langle n|k\rangle = \frac{1}{\sqrt{N}} e^{ikn}. \quad (\text{B4})$$

The general state at any time-step t is

$$\psi_{\pm}(n, t) = \frac{1}{\sqrt{N}} \sum_{k,p} e^{ikn - i\omega_p(k)t} \alpha(k, \omega_p(k)) \psi_{\pm}(k, \omega_p(k)). \quad (\text{B5})$$

Therefore

$$\begin{aligned} &\psi_+(n, t) \psi_+^*(n, t-\tau) \\ &= \frac{1}{N} \sum_{k,p} \sum_{k',p'} e^{i(k-k')n} e^{-i\omega_p(k)t} \alpha(k, \omega_p(k)) \psi_+(k, \omega_p(k)) \times \\ &\quad e^{i\omega_{p'}(k')(t-\tau)} \alpha^*(k', \omega_{p'}(k')) \psi_+^*(k', \omega_{p'}(k')). \end{aligned} \quad (\text{B6})$$

Using $\sum_{n=1}^N e^{i(k-k')n} = N\delta_{kk'}$ we get

$$\begin{aligned}
& \sum_n \psi_+(n, t) \psi_+^*(n, t - \tau) \\
&= \sum_k \left[\sum_p e^{-i\omega_p(k)t} \alpha(k, \omega_p(k)) \psi_+(k, \omega_p(k)) \right] \times \\
& \quad \left[\sum_{p'} e^{i\omega_{p'}(k)(t-\tau)} \alpha^*(k, \omega_{p'}(k)) \psi_{p'}^*(k, \omega_{p'}(k)) \right] \\
&= \sum_k \sum_p e^{-i\omega_p(k)\tau} |\alpha(k, \omega_p(k))|^2 |\psi_+(k, \omega_p(k))|^2 \\
& \quad + \sum_k \sum_{p \neq p'} e^{-i\omega_p(k)t} \alpha(k, \omega_p(k)) \psi_+(k, \omega_p(k)) \times \\
& \quad e^{i\omega_{p'}(k)(t-\tau)} \alpha^*(k, \omega_{p'}(k)) \psi_{p'}^*(k, \omega_{p'}(k)) . \quad (\text{B7})
\end{aligned}$$

Averaging over the time steps t leads to a vanishing of the cross terms in Eq. (B7) since

$$\lim_{T \rightarrow \infty} \frac{1}{T} \sum_{t=0}^T e^{\pm i[\omega_-(k) - \omega_+(k)]t} = \delta_{\omega_+(k) \omega_-(k)} = 0, \quad (\text{B8})$$

where T is also a multiple of m . Therefore we arrive at

$$\begin{aligned}
C_M(\tau) &= \lim_{T \rightarrow \infty} \frac{1}{T} \sum_{t=0}^T C_M(t, \tau) \\
&= \sum_k \sum_{p=\pm} e^{-i\omega_p(k)\tau} |\alpha(k, \omega_p(k))|^2 |\psi_+(k, \omega_p(k))|^2 \\
& \quad - e^{-i\omega_p(k)\tau} |\alpha(k, \omega_p(k))|^2 |\psi_-(k, \omega_p(k))|^2 . \quad (\text{B9})
\end{aligned}$$

Applying a discrete Fourier transform from the time do-

main τ to the frequency domain ω we arrive at

$$\begin{aligned}
C_M(\omega) &= \lim_{T \rightarrow \infty} \frac{1}{T} \sum_{\tau=0}^T e^{i\omega\tau} C_M(\tau) \\
&= \sum_l |\alpha(k_l, \omega)|^2 |\psi_+(k_l, \omega)|^2 - |\alpha(k_l, \omega)|^2 |\psi_-(k_l, \omega)|^2 \\
&= \sum_l |\alpha(k_l, \omega)|^2 M(k_l) . \quad (\text{B10})
\end{aligned}$$

In Eq. (B10) the last sum runs over all such k_l which yield the same frequency ω . If the initial state was a superposition of all basis states with coefficients whose absolute values are equal, such that

$$|\alpha(k, \omega_+(k))| = |\alpha(k, \omega_-(k))| = \frac{1}{\sqrt{2N}} \quad \text{for all } k \quad (\text{B11})$$

we finally obtain

$$C_M(\omega) = \frac{1}{2N} M_s(\omega) . \quad (\text{B12})$$

Note that the assumption of all basis states having the same weight is similar to a generalized notion of infinite temperature. In other words $C_M(\tau)$ will be the expectation value of the operator $(U^{(m)})^{\tau/m} \cdot \hat{M}$ w.r.t. a density matrix $\rho = \sum_k \sum_p |k\rangle \langle k| \otimes |\psi(k, \omega_p(k))\rangle \langle \psi(k, \omega_p(k))|$. The ρ is diagonal in eigenbasis with uniform probabilities, and hence it describes a thermal state at infinite temperature limit. The proposed measurement is therefore expected to be capable of detecting a symmetry breaking in the evolution of a quantum Floquet system at infinite temperature.